Incorporation of Inorganic Anions in Calcite

Jasminka Kontrec,[a] Damir Kralj,*[a] Ljerka Brečević,[a] Giuseppe Falini,[b] Simona Fermani,[b] Vesna Noethig-Laslo,[c] and Krunoslav Mirosavljević[c]

Keywords: Anions / Calcite / Calcium carbonate / Crystal growth / EPR spectroscopy

A number of analytical methods and techniques (X-ray diffraction, FT-IR and electron paramagnetic resonance spectroscopy, ionic chromatography, scanning electron microscopy, etc.) have been used to study the mode and sites of incorporation of some common inorganic anions (SO_4^{2-}, NO_3^- and Cl^-) in the calcite crystal lattice. Calcite, the thermodynamically stable calcium carbonate polymorph under standard conditions, was prepared by spontaneous precipitation from calcium hydroxide and carbonic acid solutions. The particular co-anion was added into the carbonic acid solution in the form of a calcium salt before mixing the reactants. The system prepared in such a way is particularly suitable for investigating the mode of foreign anion incorporation into the crystal lattice of calcite. Apart from the constituent ions and the products of water protolysis, this system contains only the co-anion examined. In order to study the local environment in the calcite crystal lattice by EPR spectroscopy, Mn^{2+} was used as a paramagnetic substitute for Ca^{2+}. The experiments were performed at 25 °C and the samples for analyses were taken after a predetermined ageing time of 20 min. It was found that the co-anions, when added in the concentrations examined, did not affect the morphology of the calcite crystals but were incorporated into the calcite structure. The largest distortion of the calcite structure was obtained when sulfate ions were added. The measured parameters of the calcite unit cell are given, the results obtained are discussed and a model that explains the possible mode and sites of sulfate incorporation is presented.

Introduction

In a previous paper, a whole range of different thermodynamic and hydrodynamic parameters that could influence physical-chemical properties of the precipitated calcium carbonate was investigated.[1] Different processes were involved in its formation and different products (polymorphs) were obtained. Thus, even in the systems in which calcite was found to be the only solid phase after the predetermined period of time, its formation was the result either of the recrystallisation of the precursor phase(s) (amorphous calcium carbonate, vaterite) or the crystallisation. As a consequence, the calcite crystals appeared with a range of different physical properties (morphology, size etc.). The influence of foreign ions, primarily Mg^{2+}, in conjunction with some common anions (SO_4^{2-}, NO_3^- and Cl^-) on the physical and chemical properties of calcium carbonate precipitate was also described. The aim of these investigations was principally to study the effects of both the cation and the anions on the morphology of calcite. This work showed that incorporation of magnesium into the calcite crystal lattice depends on the nature of the co-anion present in the system. It was also shown that there is a clear relation between the morphological properties of calcites containing magnesium and the concentration of the corresponding anion, as well as the amount of Mg^{2+} incorporated into calcite lattice. Besides, it was found that the addition of sulfate ions only, caused the formation of spherical aggregates of the originally rhombohedral calcite crystals. Calcite was chosen because it is the only thermodynamically stable polymorph of calcium carbonate under standard conditions to which the other two less stable polymorphs (aragonite and vaterite) gradually transform. Moreover, extensive data relating to calcite exist in the literature. These data are the source of valuable information necessary for our findings to be explained and for the model proposed, in which small inorganic anions are incorporated into the calcite lattice. In addition, calcite is of great interest because of its wide use in industry (pigment and filler in paper, rubber, plastics, paints etc.) and also because of its widespread occurrence in the natural environment (biomineralisation, geological scales). It also has significant impact on energy production and water treatment (scaling). In all these instances, the crystal size distribution and morphology of the crystals are of great significance, as well as their chemical composition

[a] Laboratory for Precipitation Processes, Division of Materials Chemistry, Ruđer Bošković Institute,
P. O. Box 180, 10002 Zagreb, Croatia
Fax: (internat.) + 385-1-4680098
E-mail: kralj@rudjer.irb.hr
[b] Dipartimento di Chimica "G. Ciamician", Università degli Studi,
via Selmi 2, 40126 Bologna, Italy
[c] Laboratory for Magnetic Resonance, Division of Physical Chemistry, Ruđer Bošković Institute,
P. O. Box 180, 10002 Zagreb, Croatia

(degree of the additive incorporation into the crystal lattice). Additives and impurities of both an inorganic and an organic nature play an important role. In recent years, the most intensively investigated additives concerning this matter were soluble polymeric and special functional low molecular weight additives,[2−7] as well as the protein macromolecules isolated from some living organisms.[8−11] Among the inorganic ions and small molecules, the effects of Mg^{2+} and some organic acids[12−19] on the formation and morphology of calcium carbonate polymorphs were studied much more than the effects of anions and other cations.[1,20−23] Only a few papers[1,20,22] have considered anions as a possible way of controlling the calcite morphology. The anions studied in our previous investigations and in the present work were chosen because they are the possible impurities in any precipitation system and some of them, such as SO_4^{2-} in seawater, can be present in rather high concentrations.

In order to investigate the role of anions separately from the foreign cations in the calcium carbonate precipitation system in this investigation, calcite was precipitated from a system in which calcium hydroxide and carbonic acid solutions were used as reactants. Thus, any possible effects of ions other than the constituent ions or products of autoprotolysis of water (Ca^{2+}, CO_3^{2-}, HCO_3^-, H_3O^+, OH^-) on the precipitation of calcite were avoided. Calcite prepared in such a way can be used as a reference material for a number of different studies. After that, foreign anions were added to the precipitation system in the form of calcium salts [$CaSO_4$, $Ca(NO_3)_2$ and $CaCl_2$] and a relatively narrow range of the co-anion concentrations was investigated at a relatively low initial supersaturation.

The aim of the present work was to shed more light upon the mode and sites of incorporation of these anions into the calcite lattice. For this purpose X-ray powder diffraction (XRD), FT-IR and electron paramagnetic resonance (EPR) spectroscopy, scanning electron microscopy (SEM) and ion chromatography (IC) were used. In order to study the local environment in the calcite crystal lattice by EPR spectroscopy, Mn^{2+} was used as a paramagnetic substitute for Ca^{2+}. Mn^{2+} is a particularly appropriate probe for such a study because it readily substitutes for Ca^{2+} in the calcite structure and gives a strong EPR signal at room temperature providing abundant information even in the solid state.[13,24−29]

Results and Discussion

All experiments were performed on the precipitation system in which the total initial concentrations of calcium and carbonate ions in solution were, respectively, $c_i(Ca^{2+}) = 5.0 \times 10^{-3}$ mol·dm^{-3} and $c_i(CO_3^{2-}) = 9.0 \times 10^{-3}$ mol·dm^{-3} and the initial pH was approximately 8.7. The initial supersaturation of this system $S = (\Pi/K_{sp}^{o})^{1/2}$, defined as relative supersaturation, S-1, where Π is the ion activity product $\Pi = a(Ca^{2+})\cdot a(CO_3^{2-})$ and K_{sp}^{o} is the thermodynamic equilibrium constant of calcite dissolution ($K_{sp}^{o} = 3.313 \times 10^{-9}$ at 25 °C), was calculated to be S-1 = 10.38. The detailed calculation procedure, which takes into account the respective protolytic equilibria and equilibrium constants as well as the charge and mass balance equations, has been given previously.[1,30]

Figure 1 (a) shows typical crystal size distributions of calcite precipitated in a pure system. A relatively narrow distribution was obtained exhibiting a maximum at about 7 μm. This is consistent with the previous findings[1] according to which the crystals obtained at relatively low supersaturations [(S-1) < 20], formed by heterogeneous nucleation and slow crystal growth, are small in size and considerably monodispersed. This also confirms the observation that the crystal size distribution depends primarily on supersaturation and not on the initial molar ratios $c_i(Ca^{2+})/c_i(CO_3^{2-})$, since such distributions are obtained regardless of carbonate or calcium ions being in excess in the system. The presence of a co-anion (sulfate, nitrate, chloride), added in the system in concentrations mentioned above, did not change the size distribution significantly. Figure 1 (b) shows such a distribution obtained when the highest of the $CaSO_4$ concentrations examined in this work ($c_i = 1.0 \times 10^{-3}$ mol·dm^{-3}) was added into the precipitation system. Slight differences between the distribution curves shown in Figure 1 (a and b) reflect the appearance of a certain portion of smaller calcite crystals obtained in the system with the additive.

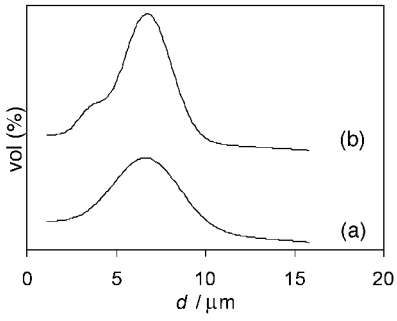

Figure 1. Volume distributions of calcite crystals obtained in the precipitation system $c_i(Ca^{2+}) = 5.0 \times 10^{-3}$ mol·dm^{-3}, $c_i(CO_3^{2-}) = 9.0 \times 10^{-3}$ mol·dm^{-3} at 25 °C, containing $CaSO_4$: a) 0 mol·dm^{-3}; b) 1.0×10^{-3} mol·dm^{-3}

Rather uniformly shaped crystals were obtained with or without the addition of the co-anions. As an example, Figure 2 shows scanning electron micrographs of calcite crystals obtained in the systems with increasing concentrations of sulfate ions. At the highest concentration of sulfate ions, a slight tendency towards the formation of aggregates of smaller rhombohedral calcite crystals, as shown in Figure 2 (d), could be sporadically observed. This is consistent with the findings represented in Figure 1. It should be noted that the effect of sulfate ions on the calcite morphology is more pronounced in the precipitation systems, in which the initial supersaturation, and consequently the growth rate and the aggregation tendency is much higher (S-1 > 30, pH_i > 10.5). In such cases, the formation of spherical aggregates

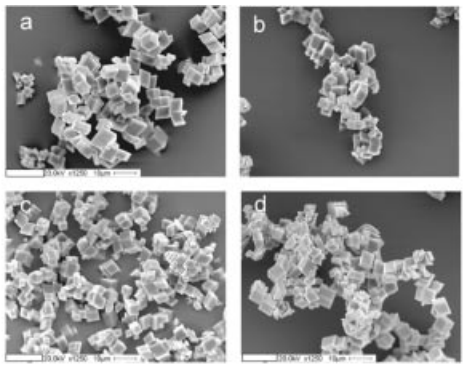

Figure 2. Scanning electron micrographs of calcite crystals isolated from the system $c_i(Ca^{2+}) = 5.0 \times 10^{-3}$ mol·dm^{-3}, $c_i(CO_3^{2-}) = 9.0 \times 10^{-3}$ mol·dm^{-3} at 25 °C, to which the following concentrations of $CaSO_4$ were added: (a) 1.0×10^{-4} mol·dm^{-3}, (b) 3.0×10^{-4} mol·dm^{-3}, (c) 6.0×10^{-4} mol·dm^{-3} and (d) 1.0×10^{-3} mol·dm^{-3}

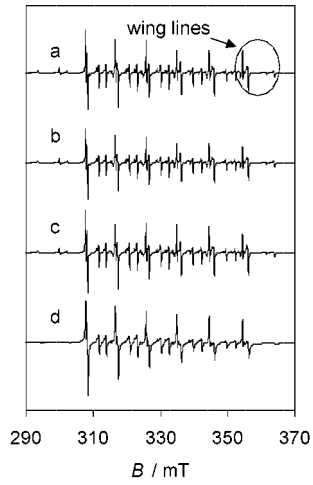

Figure 3. EPR spectra of $^{55}Mn^{2+}$ in (a) pure calcite (the "wing lines" are denoted) and calcites prepared in the presence of 1.0×10^{-3} mol·dm^{-3}: (b) NO_3^-, (c) Cl^- and (d) SO_4^{2-}; the measured parameters of the spectra are given in Table 1

of the originally rhombohedral calcite crystals could be obtained.[1] In order to minimise the influence of the kinetic factors, a relatively narrow range of the co-anion concentrations was investigated at a relatively low initial supersaturation. Such precautions were necessary since changes in nucleation and/or crystal growth rates can cause changes in the growth mechanisms and, consequently, influence the mode and extent of the co-anion incorporation. Therefore, the initial supersaturations in the systems with and without the addition of co-anions were also kept approximately the same.

In order to establish the possible incorporation of sulfate into the calcite lattice and to find out the possible sites and mode of their incorporation, the samples were analysed by EPR spectroscopy, IC and XRD. Figure 3 shows a comparison of an EPR spectrum of Mn^{2+}-doped pure calcite (spectrum a) with the EPR spectra of Mn^{2+}-doped calcite samples obtained when the highest concentration of co-anions used in this work were added to the precipitation system, i.e. 1.0×10^{-3} mol·dm^{-3} NO_3^- (spectrum b), 1.0×10^{-3} mol·dm^{-3} Cl^- (spectrum c) or 1.0×10^{-3} mol·dm^{-3} SO_4^{2-}, (spectrum d). The lines in spectrum b remain similar in structure and linewidth to those in spectrum a. Spectra c and d exhibit broader lines and a larger broadening of the wing lines. Results of the EPR spectroscopic analyses are summarised in Table 1. It can be seen that the addition of Cl^- or SO_4^{2-} is reflected in the spectra as an increase in the parameter D' from 1.7 mT to 1.8 mT. On the other hand, the addition of NO_3^- did not show any effect of this kind. Parameter D' reflects the distortion of the calcite lattice from axial symmetry. The increase of D' may be accompanied by the uniaxial strain of the threefold axis, expressed in the EPR spectra by broadening of the wing lines (*RH* parameter). Uniaxial strain is produced by defects in the crystal lattice due to the different charges or sizes of the impurity ions, the co-anions in this case. Any of these cannot affect the spectroscopic hyperfine linewidths (ΔW). The *RH* parameters measured in the samples to which SO_4^{2-}, Cl^- or NO_3^- were added are displayed in Figure 4 as a function of the co-anion initial concentrations. A pronounced increase in the *RH* parameter upon the addition of SO_4^{2-} suggests that although these anions match the charge of the calcite CO_3^{2-} groups, they produce

Table 1. EPR spectroscopic parameters [axial unit cell distortion, D'; parallel ($\Delta W_\parallel$) and perpendicular ($\Delta W_\perp$) hyperfine linewidths of $m_{Mn} = -5/2$; "wing lines" broadening, *RH*] of pure calcite and calcite samples prepared with the addition of different concentrations of Cl^-, NO_3^- and SO_4^{2-} ions

	c [mol·dm^{-3}]	D' [mT]	$\Delta W_\parallel$ [mT]	$\Delta W_\perp$ [mT]	P	Q	$RH = P/Q$
	0	1.72 ± 0.02	0.17 ± 0.02	0.24 ± 0.03	1853.0	290.3	6.4
Chloride	0.0010	1.80 ± 0.05	0.20 ± 0.03	0.26 ± 0.03	1760.8	221.2	8.0
	0.0006	1.80 ± 0.05	0.15 ± 0.03	0.23 ± 0.03	1681.4	233.5	7.2
	0.0003	1.80 ± 0.05	0.16 ± 0.03	0.22 ± 0.03	1189.8	182.3	6.5
Nitrate	0.0010	1.71 ± 0.02	0.19 ± 0.02	0.25 ± 0.03	990.0	158.2	6.3
	0.0006	1.79 ± 0.02	0.20 ± 0.02	0.26 ± 0.03	978.0	163.8	6.0
	0.0003	1.71 ± 0.02	0.18 ± 0.02	0.24 ± 0.03	1550.0	240.6	6.4
	0.0001	1.74 ± 0.02	0.15 ± 0.02	0.25 ± 0.03	1161.4	192.0	6.0
Sulfate	0.0010	1.82 ± 0.05	0.24 ± 0.03	0.41 ± 0.03	577.4	11.1	52.0
	0.0006	1.82 ± 0.05	0.24 ± 0.03	0.35 ± 0.03	530.0	15.2	34.9
	0.0003	1.80 ± 0.05	0.18 ± 0.03	0.27 ± 0.03	635.6	32.4	19.6
	0.0001	1.71 ± 0.03	0.21 ± 0.03	0.24 ± 0.03	962.0	84.2	11.4

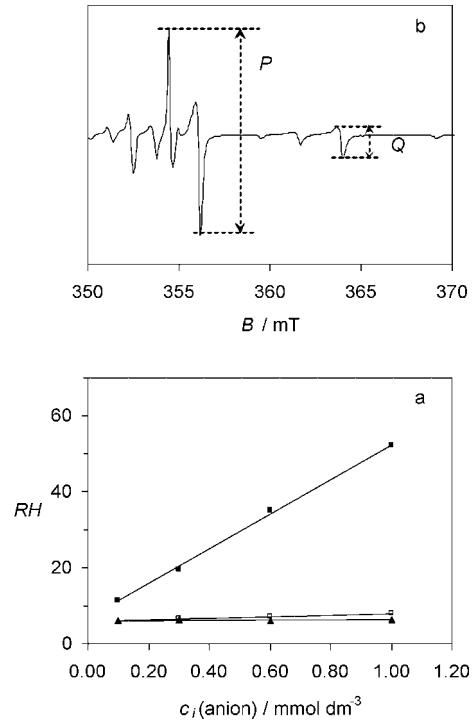

Figure 4. Plots of the *RH* parameter, broadening of the wing lines in the EPR spectrum, as a function of co-anion concentration (a): sulfate (solid squares), chloride (open squares) and nitrate (solid triangles); the *P* and *Q* parameters are denoted on the magnified image of the wing lines shown in Figure 3 (b); from these parameters $RH = P/Q$ was calculated

larger uniaxial strain than NO_3^- or Cl^-. As uniaxial strain has its effect on the threefold axis of the crystal symmetry alone, one would expect it to have a larger effect on the symmetry of only one of the crystal axes, that is, along the *c* axis of the calcite lattice.

Figure 5 compares the X-ray diffraction pattern of pure calcite with those of the samples prepared with the addition of the highest concentration (1.0×10^{-3} mol·dm^{-3}) of co-anions examined in this work. All the diffraction patterns reveal the presence of calcite as the unique calcium carbonate crystalline phase. It is evident that the presence of nitrate ions in the precipitation system does not have an effect on the diffraction pattern of the precipitated calcite which is similar to that of pure calcite. The presence of chloride ions also has no effect on the diffraction peak positions but results in a slight increase of the diffraction peak full width half maxima (FWHM) as the co-anion concentration increases. Since this effect indicates a reduction in the overall crystallinity, it could be related to the incorporation of chloride ions into the calcite structure. The effect of sulfate ions is more pronounced. These ions are not only incorporated in the calcite structure but, at the same time, they induce a reduction in the phase crystallinity. Although the differences among the diffraction patterns presented are minimal, they can be considered as relevant because the trend in the increase of line broadening follows the increase of the initial co-anion concentration in solution.

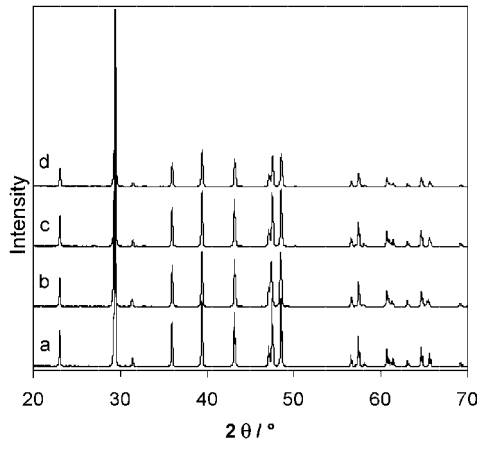

Figure 5. Powder X-ray diffraction pattern of (a) pure calcite and calcites prepared in the presence of 1.0×10^{-3} mol·dm^{-3}: (b) sulfate, (c) nitrate and (d) chloride

Additional support to the previous conclusions is provided by the differential thermal analyses (DTA) of the samples. An endothermic peak at 810 °C was obtained for pure calcite, denoting its decomposition by loss of CO_2. The samples prepared with the addition of 1.0×10^{-3} mol·dm^{-3} $CaSO_4$ showed a shift in this peak by 15 °C toward lower temperatures. These observations suggest that such a shift could be induced by incorporation of sulfate ions in the calcite structure causing a destabilising effect.

Since SO_4^{2-} showed the largest effect on the calcite crystal symmetry, most emphasis will be given to this anion in the following discussion.

Figure 6 shows the content of sulfate ions in the calcite crystals, determined by ion chromatography, as a function of the initial concentration of sulfate ions in the precipitation systems. The incorporation of sulfate ions in the solid phase increases linearly with the increase in the amount of $CaSO_4$ added. This is consistent with the XRD measurements of the calcite unit cell parameters (i.e. *a*, *c* and unit cell volume), as shown in Table 2. The changes in the *a* and *c* axes are also linearly dependent on the quantity of sulfate ions added to the precipitation systems, the change in the *c* axis being larger than that in *a* axis. Figure 7 shows these changes as a relative scale, i.e. as $(a_{sample}/a_{reference}) \times 100$.

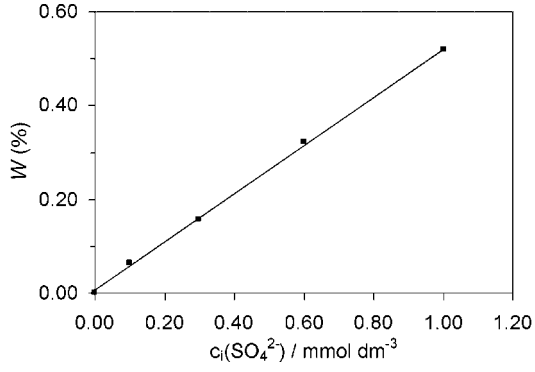

Figure 6. Sulfate ion content in the calcite crystals, determined by ion chromatography, as a function of the initial concentration of sulfate ions added as $CaSO_4$ in the precipitation systems

Table 2. Calcite unit cell parameters and full width half maxima (FWHM) of two diffraction peaks as a function of sulfate ion concentration added to the precipitation system

Sample	$c_i(SO_4^{2-})$ [mmol·dm^{-3}]	a [Å]	c [Å]	V [Å^3]	FWHM (006)[a] (2θ)	FWHM (300)[a] (2θ)
Ref. data[31]		4.989	17. 062	367.78		
00[b]	0.00	4.9917(2)	17.069(9)	368.34(3)	0.09	0.10
S 01	0.10	4.9899(1)	17.085(5)	368.43(1)	0.12	0.10
S 02	0.30	4.9931(2)	17.081(8)	368.8(3)	0.12	0.10
S 03	0.60	4.99258(7)	17.10(1)	369.2(9)	0.13	0.11
S 04	1.00	4.996(4)	17.11(1)	370.0(5)	0.15	0.13

[a] Miller index of the calcite structure according to a rhombohedral unit cell.[31] [b] Pure calcite obtained from the precipitation system.

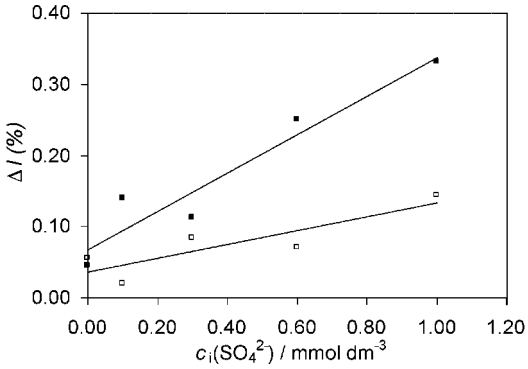

Figure 7. Relative changes of calcite crystal cell *a* (open squares) and *c* (solid squares) axes shown as a function of the initial concentration of sulfate ions added as $CaSO_4$, in the precipitation systems

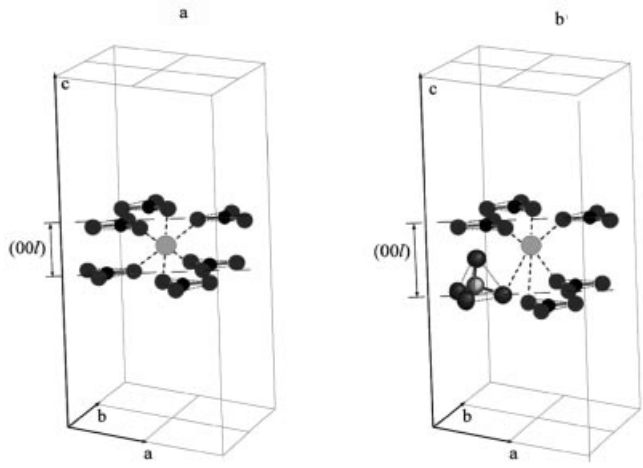

Figure 8. Schematic representation of the model showing: (a) the calcite crystal lattice cell and (b) the possible mode and site of sulfate ion incorporation

The observed similarity in the crystal size distributions (Figure 1) and morphologies (Figure 2) of the investigated systems, as well as the linear dependence of the amount of anion incorporated in the calcite crystals on its concentration in solution (Figure 6), give additional assurance that the extent and mode of anion incorporation (SO_4^{2-} in particular) are predominantly functions of thermodynamic factors (e.g. chemical nature of the ions, ionic radii, coordination properties, hydration free energy etc.).

Based on the results of EPR spectroscopic, IC and particularly the XRD analyses, a simplified model can be proposed which attempts to explain the mode and site of sulfate incorporation in the calcite crystal lattice. A schematic presentation of a calcite crystal lattice, in which one calcium ion is coordinated with six carbonate ions, is shown in Figure 8 (a). If a planar carbonate is replaced by a sulfate ion, three of the sulfate's apical oxygen atoms in the tetrahedral structure could be accommodated in the place of the planar trigonal carbonate, as shown in Figure 8 (b). In this case, the sulfur and the fourth oxygen atom of the sulfate are out of the carbonate plane which induces an increase in the calcite *c* axis. A small increase in the *a* axis can also be expected, since the three apical oxygen atoms of the sulfate occupy a slightly larger surface (256.4 Å^2) in the plane compared with the carbonate ion (212.1 Å^2). In accordance with the proposed model, the effect of distortion of the calcite structure, caused by sulfate substitution, should be more evident along the *c* axis. At the highest isomorphic substitution of sulfate ions obtained, the distortion of the unit cell axes, with respect to the pure calcite, was about 0.05 Å (0.3%) and 0.01 Å (0.1%) for the *c* and *a* axes, respectively. The XRD broadening of peaks, detected in the calcite samples prepared with the additions of sulfate ions, confirms the crystal lattice disorder induced by the presence of sulfate ions (Table 2). This effect, related to the size of the crystalline domains, is quite evident in the (00*l*) reflections but is smaller in the (*h*00) reflections. This suggests a higher degree of disorder induced in the calcite structure by sulfate ions along the *c* direction.

These crystallographic observations agree well with the EPR spectroscopy and provide evidence of the importance of the sulfate ions in destabilising the calcite structure.

Conclusions

The extent and mechanism of incorporation of some common inorganic anions (SO_4^{2-}, Cl^-, NO_3^-) into the calcite crystal lattice and their influence on the physical and chemical properties of the precipitate were investigated in the precipitation system under conditions of a moderate relative initial superstaturation (S-1 = 10.4) at 25 °C.

In order to avoid the presence of any undesirable chemical species (except Ca^{2+}, CO_3^{2-} and the products of their hydrolysis, as well as H^+ and OH^-) the precipitation was

initiated by mixing calcium hydroxide ($c_i = 5.0 \times 10^{-3}$ mol·dm^{-3}) and carbonic acid ($c_i = 9.0 \times 10^{-3}$ mol·dm^{-3}) solutions. For the same reasons, no pH or ionic strength adjustments were made.

Under the given experimental conditions, calcite crystals were formed by heterogeneous nucleation and were small in size and considerably monodispersed.

The co-anions (chloride, nitrate or sulfate) were added into the system in the form of an appropriate calcium salt and the addition of any of the co-anions did not cause significant changes in the physical or chemical properties of the precipitate.

According to the X-ray diffraction, ion chromatographic and EPR spectroscopic analyses of the calcite samples, the respective co-anions were incorporated into the calcite crystal lattice to a certain extent, the incorporation of sulfate ions being the most extensive.

A model of sulfate incorporation into the calcite lattice can be proposed: carbonate ions are partially substituted by sulfate ions, thus causing a distortion of the calcite unit cell. The degree of disorder along the *c* axis is much higher than along the other two crystallographic directions as a consequence of substitution of the tetrahedral sulfate for the planar carbonate ions.

Experimental Section

Materials: All solutions used were prepared from analytically pure chemicals and deionised water of high quality (conductivity < 0.1 μS·cm^{-1}). For the experiments, a thermostatted double-walled glass vessel of 400 mL capacity was used. Precipitation of calcite was initiated by pouring 150 mL of carbonic acid solution into the same volume of calcium hydroxide solution of the appropriate concentration. During precipitation, the system was continuously stirred at a constant rate by means of a flat-bladed stirrer with two perpendicular blades and the extent of the reaction was determined by measuring the pH of the solution. All experiments were performed at 25 °C.

The carbonic acid stock solution was prepared by bubbling a high-grade carbon dioxide stream into water until the apparent constancy of the pH was obtained. The exact concentrations of freshly prepared carbonic acid stock solutions were determined by potentiometric titration using a standard NaOH solution ($c = 0.10$ mol·dm^{-3}). The calcium hydroxide stock solution was prepared by adding an excess of calcium hydroxide into water. The suspension was then filtered through a 0.22 μm membrane filter and the saturated solution was kept under nitrogen. The exact concentration was determined by potentiometric titration using a standard HCl solution ($c = 0.10$ mol·dm^{-3}) and the total calcium content was additionally checked by complexometric titration with EDTA. Foreign anions were added to the system in the form of a calcium salt (calcium sulfate, calcium nitrate or calcium chloride). The required amount of the foreign anion was always added into the freshly prepared carbonic acid solution of known concentration [$c_i(CO_3^{2-}) = 9.0 \times 10^{-3}$ mol·dm^{-3}, diluted from the stock solution] and the total initial concentration of the foreign anion in the system was varied [c_i(anion) = 1.0×10^{-4}, 3.0×10^{-4}, 6.0×10^{-4} or 1.0×10^{-3} mol·dm^{-3}]. The total initial calcium concentration in the system was kept the same [$c_i(Ca^{2+}) = 5.0 \times 10^{-3}$ mol·dm^{-3}] in all experiments.

The samples for analyses were taken after a predetermined ageing time of 20 min, when the total volume of suspension was filtered through a 0.22 μm membrane filter, thoroughly washed with small portions of water and dried at 105 °C. In the system in which no additive was added [$c_i(Ca^{2+}) = 5.0 \times 10^{-3}$ mol·dm^{-3} and $c_i(CO_3^{2-}) = 9.0 \times 10^{-3}$ mol·dm^{-3}], the precipitate consisted entirely of calcite crystals and the amount of crystals obtained in one preparation was just sufficient for all types of analyses to which the solid phase was subjected to.

Methods: The precipitate composition was characterised by a combination of FT-IR spectroscopic (Mattson), thermogravimetric (Mettler TG 50 thermobalance with TC 11 TA processor), differential thermal (Netzsch differential thermal analyzer), and scanning electron microscopic (Philips XL-20) analyses. TGA and DTA were carried out with a heating rate of 20 °C/min and 10 °C/min, respectively, and Al_2O_3 was used as the reference substance for DTA. For the SEM observations, the dried samples were glued by a carbon tape on an aluminium stub and were gold-coated.

Crystal number and size distributions were determined by means of an electronic counting device (Coulter Electronics Ltd.) fitted with a 50-μm orifice tube. This aperture-size diameter enabled crystals in the size range between about 1 and 30 μm to be measured. The instrument was calibrated with standard latex spheres (13.3 μm in diameter). The total content of calcium and sulfate ions in the solid phase was determined by means of an ionic chromatography system (Dionex DX100 fitted with a CD20 conductivity detector). The chromatographic data were collected and processed with the Dionex Peaknet 5.1 program.

The possible incorporation of the co-anion into the calcite structure was evaluated by measuring the calcite unit-cell parameters by XRD. The sample for the X-ray data collection was manually ground in an agate mortar. The powder was mounted on a 1.5 mm thick flat Al holder using the front loading technique and the data collection was performed using a powder diffractometer (Philips PW 1050/81 equipped with a secondary graphite monochromator; Cu-K_α radiation at 40 kV and 40 mA). The instrument was configured with a 1° divergence and 0.2 mm receiving slits. The presence of impurities was checked and excluded by a preliminary qualitative analysis of the X-ray powder pattern. The phase identification was possible using the ICDD-PDF-2 database.[32] The unit cell parameters and their standard deviations were calculated using the CellSize computer program.[33] The number of significant figures of the data obtained depends on the material crystallinity. The diffraction peak full width half maxima (FWHM) were calculated using the computer program WinFit.[34]

Apart from XRD, the interaction of foreign anions with the calcite crystals was also studied by EPR spectroscopy (Varian E-9 spectrometer equipped with a dual microwave resonant cavity). In this case, the local environment of Ca^{2+} in the crystal lattice of calcite was studied using Mn^{2+} ions as a paramagnetic substitute for Ca^{2+}. The calcite crystals were prepared by adding carbonic acid solution (150 mL of 9.0×10^{-3} mol·dm^{-3}) into an equal volume of calcium hydroxide solution (5.0×10^{-3} mol·dm^{-3}). Manganese (2.0×10^{-7} mol·dm^{-3}) was added into the carbonic acid solution prior to mixing the reactants, so that the Mn^{2+} substitution for Ca^{2+} took place during the precipitation of calcite.[13] After the initial mixing of the reactants, the system was agitated mechanically with a flat-bladed stirrer for 20 min at a constant rate and then aged for 30 d without further stirring. The calcite thus obtained was filtered, washed several times with small portions of water, dried at 105 °C and stored in a desiccator. The EPR spectrum of such Mn^{2+}-doped calcite crystals was used as a reference. The uptake of Mn^{2+} by such a method (as determined by IC) was approxi-

mately 0.005 mol%.[13] This amount does not cause any measurable change in the unit cell parameters of calcite. This was established by our own XRD analyses and has also been reported by other researchers.[29] A qualitative interpretation of the EPR spectroscopic parameters proposed by Angus et al.[29] was applied. These authors reported that the axial distortion parameter D' of the calcite unit cell depends on temperature, pressure and the concentration and nature of the impurity ions incorporated into calcite. In a magnetic field and in the absence of any ligands, Mn^{2+} ions give six lines in the EPR spectrum due to the hyperfine interaction of the high-spin electron state of five electrons, $S = 5/2$, with the nuclear spin of $^{55}Mn^{2+}$ nuclei, $I = 5/2$. The crystal field of the CO_3^{2-} ligands in the calcite unit cell splits these spectral lines further, giving rise to a multi-line EPR spectrum. Thus, the spectrum contains information about the CO_3^{2-} symmetry in the calcite lattice. Any axial distortion of the CO_3^{2-} ligands around Mn^{2+} in the calcite lattice changes the crystal field parameter D' in the spectrum. This parameter is best regarded as a measure of the separation of the parallel and perpendicular components of each of the six main hyperfine lines in the EPR spectrum of calcite and is largest for the high-field hyperfine line $m_{Mn} = -5/2$. The line shapes, ΔW, of the Mn^{2+} spectra are expected to be Lorenzian because of homogeneous line-broadening. Deviations from these ideal line shapes, giving rise to an inhomogeneous line broadening, can be caused by many factors. As suggested by Barberis et al.,[28] a random distribution of oxygen atoms of the CO_3^{2-} groups about their equilibrium positions in the calcite lattice can be induced by the impurity ions. In the EPR spectra, this is reflected as a broadening of all spectral lines and is measured by the parallel ($\Delta W_{\|}$) and perpendicular ($\Delta W_{\perp}$) linewidths of the hyperfine line $m_{Mn} = -5/2$ at half-height from the baseline. On the other hand, the compression along the threefold axis, or random electric fields produced by impurities with different charges or sizes, cannot affect the linewidth of the main lines but does broaden the outer so called "wing lines".[29] This is expressed as the so-called *RH* parameter.

Acknowledgments

This research has been sponsored by the Ministry of Science, Education and Sport of the Republic of Croatia (Project No. 0098061).

[1] D. Kralj, J. Kontrec, Lj. Brečević, G. Falini, V. Nöthig-Laslo, *Chem. Eur. J.* **2004**, *10*, 1647−1656.
[2] J. M. Didymus, P. Oliver, S. Mann, A. L. DeVries, P. V. Hauschka, P. Westbroek, *J. Chem. Soc., Faraday Trans.* **1993**, *89*, 2891−2900.
[3] L. A. Gower, D. A. Tirrel, *J. Cryst. Growth* **1998**, *191*, 153−160.
[4] S. K. Zhang, K. E. Gonsalves, *Langmuir* **1998**, *14*, 6761−6766.
[5] G. Xu, N. Yao, I. A. Aksay, J. T. Groves, *J. Am. Chem. Soc.* **1998**, *120*, 11977−11985.
[6] K. Naka, Y. Tanaka, Y. Chujo, Y. Ito, *Chem. Commun.* **1999**, 1931−1932.
[7] J. García-Carmona, J. Gómez-Morales, J. Fraile-Sainz, R. Rodrígez-Clemente, *Powder Technol.* **2003**, *130*, 307−315.
[8] G. Falini, S. Albeck, S. Weiner, L. Addadi, *Science* **1996**, *271*, 67−69.
[9] N. Wada, K. Yamasita, T. Umegaki, *J. Colloid Interface Sci.* **1999**, *212*, 357−364.
[10] A. M. Belcher, X. H. Wu, R. J. Christensen, P. K. Hansma, G. D. Stucky, D. E. Morse, *Nature* **1996**, *381*, 56−58.
[11] J. Aizenberg, J. Hanson, T. F. Koetzle, S. Weiner, L. Addadi,, *J. Am. Chem. Soc.* **1997**, *119*, 881−886.
[12] G. Falini, M. Gazzano, A. Ripamonti, *J. Cryst. Growth* **1994**, *137*, 577−584.
[13] Lj. Brečević, V. Nöthig-Laslo, D. Kralj, S. Popović, *J. Chem. Soc., Faraday Trans.* **1996**, *92*, 1017−1022.
[14] G. Falini, S. Fermani, M. Gazzano, A. Ripamonti, *J. Mater. Chem.* **1998**, *8*, 10611065.
[15] K. J. Davis, P. M. Dove, J. J. De Yoreo, *Science* **2000**, *290*, 1134−1137.
[16] F. C. Meldrum, S. T. Hyde, *J. Cryst. Growth* **2001**, *231*, 544−558.
[17] M. Kitamura, *J. Colloid Interface Sci.* **2001**, *236*, 318−327.
[18] C. A. Orme, A. Noy, A. Wierzbicki, M. T. McBride, M. Grantham, H. H. Teng, P. M. Dove, J. J. De Yoreo, *Nature* **2001**, *411*, 775−779.
[19] E. Loste, R. M. Wilson, R. Seshadri, F. C. Meldrum, *J. Cryst. Growth* **2003**, *254*, 206−218.
[20] B. W. H. van Beest, G. J. Kramer, R. A. van Santen, *Phys. Rev. Lett.* **1990**, *64*, 1955−1958.
[21] V. Noethig-Laslo, Lj. Brečević, *J. Chem. Soc., Faraday Trans.* **1998**, *94*, 2005−2009.
[22] S. L. Tracy, D. A. Williams, H. M. Jennings, *J. Cryst. Growth* **1998**, *193*, 382−388.
[23] V. Nöthig-Laslo, Lj. Brečević, *Phys. Chem. Chem. Phys.* **1999**, *1*, 3697−3700.
[24] F. K. Hurd, M. Suchs, W. D. Hershberger, *Phys. Rev.* **1954**, *93*, 373−380.
[25] H. M. McConnell, *J. Chem. Phys.* **1956**, *24*, 904−905.
[26] C. Kikuchi, L. M. Matarrese, *J. Chem. Phys.* **1960**, *33*, 601−606.
[27] D. J. J. Kinsman, H. D. Holland, *Geochim. Cosmochim. Acta* **1969**, *33*, 1−17.
[28] G. Barberis, R. Calvo, H. G. Maldonado, C. E. Zarate, *Phys. Rev. B* **1975**, *12*, 853−860.
[29] J. G. Angus, J. B. Raynor, M. Robson, *Chem. Geol.* **1979**, *27*, 181−205.
[30] D. Kralj, Lj. Brečević, J. Kontrec, *J. Crystal Growth* **1997**, *177*, 248−257.
[31] F. Swanson, *Natl. Bur. Stand. (US)* **1953**, *51*, 359.
[32] *Powder Diffraction File 2*, International Centre for Diffraction Data, Newtown Square, Pennnsylvania, USA, **2002**.
[33] David Hay, *CELSIZ*, CSIRO Division of Material Science and Technology, Clayton, Australia.
[34] *Winfit − A Computer Program for X-ray Diffraction Line Profile Analysis*: S. Krumm, *Acta Univ. Carol., Geol.* **1994**, *38*, 253−261.

Received April 2, 2004
Early View Article
Published Online October 7, 2004

